7122

#22

Department of Agriculture
and Fisheries for Scotland

The Theory of Solid Spheres as Sonar Calibration Targets

D N MacLennan

Scottish Fisheries Research
Report Number 22 1981

ISSN 0308-8022

LIBRARY

FEB 17 1982

National Marine Fisheries Service
2570 Dole Street
Honolulu, Hawaii

Previous Scottish Fisheries Research Reports

1975

No. 1. The Aberdeen Single-Anchor Mooring
By R. Payne, 7 pp.

No. 2. The Aberdeen Shallow Water Current Meter Mooring.
By R. Payne, 13 pp.

1976

No. 3. The Bridger Version of the Gulf III High Speed Plankton Sampler.
By J.A. Adams, 42 pp.

No. 4. Some Parasites of Plaice *Pleuronectes platessa* L. in Three Different Farm Environments.
By K. McKenzie, A.H. McVicar and I.F. Waddell, 14 pp.

No. 5. Simulation of Vertical Structure in a Planktonic Ecosystem.
By J.H. Steele and E.W. Henderson, 29 pp.

No. 6. The Intertidal Fauna of Sandy Beaches — a Survey of the Scottish Coast.
By A. Eleftheriou and A.D. McIntyre, 61 pp.

No. 7. A Net Drag Formula for Pelagic Nets.
By A.J. Reid, 12 pp.

1977

No. 8. The Aberdeen Sedimentation Trap and its Moorings.
By R. Payne and J.M. Davies, 11 pp.

No. 9. A Preliminary Model of Shear Diffusion and Plankton Populations.
By G.T. Evans, J.H. Steele and G.E.B. Kullenberg, 20 pp.

No. 10. Diving Observations on the Efficiency of Dredges used in the S Scottish Fishery for the Scallop, *Pecten maximus* (L.).
By C.J. Chapman, James Mason and J.A.M. Kinnear, 16 pp.

1978

No. 11. Comparative Fishing for Flatfish using a Beam Trawl fitted with Electric Ticklers.
By P.A.M. Stewart, 10 pp.

No. 12. The Value of Direct Observation Techniques by Divers in Fishing Gear Research
By J. Main and G.I. Sangster, 15 pp.

1979

No. 13. The Occurrence of Plerocercoids of *Diphyllobothrium spp.* in Wild Cultured Salmonids from The Loch Awe Area.
By R. Wootten and John W. Smith, 8 pp.

No. 14. A Study of Bottom Trawling Gear on both Sand and Hard Ground.
By J. Main and G.I. Sangster, 15 pp.

No. 15. The Coastal Movements of Returning Atlantic Salmon, *Salmo salar* L.
By A.D. Hawkins, G.G. Urquhart and W.M. Shearer, 15 pp.

No. 16. Hydrodynamic Characteristics of Trawl Warps.
By D.N. MacLennan, 10 pp.

No. 17. Some Parasites and Diseases of Blue Whiting. *Micromesistius poutassou* (Risso), to the North and West of Scotland and at the Faroe Islands.
By K. MacKenzie, 14 pp.

The Theory of Solid Spheres as Sonar Calibration Targets

D N MacLennan

Marine Laboratory Aberdeen

Introduction

The measurement of acoustic echoes from fish is an important method for estimating fish stocks. The precision of such estimates depends inter alia upon the accuracy to which the acoustic equipment has been calibrated. Two techniques are commonly used to perform acoustic calibrations. The reciprocity technique (Urick, 1967) requires certain assumptions about the response of the transducer when transmitting and receiving, and it is difficult to achieve a calibration accuracy better than 1dB by this method. The second technique is based on the measurement of echoes from a standard target, normally a sphere, and the response of the sonar is deduced from a knowledge of the acoustic properties of the target. Clearly the accuracy in this case depends upon how well these properties are known. However, the usual experimental approach is to measure the target properties using another transducer which has itself been calibrated by reciprocity. Therefore, to improve the calibration accuracy, some other means is required for estimating the acoustic properties of standard targets.

Welsby and Hudson (1972) suggested that ping-pong balls could be used for calibrating sonars. The stability of such targets is in doubt, however, and it is now considered that solid spheres offer a better prospect as standard targets with stable properties. This paper shows how scattering theory may be applied to estimate the target strength of solid spheres. The theory of acoustic scattering by a rigid sphere has been described by Rudgers (1969). The scattering properties of a real sphere which has finite density and elasticity are quite unlike the rigid ideal, especially above a critical frequency when the mechanical resonances of the sphere become important. Both transverse and longitudinal sound waves propagate within the sphere. Two waves propagate in the surrounding medium, namely the incident wave and the scattered wave caused by the presence of the sphere. The interaction between the various waves results in a complicated scattered sound field that is highly frequency dependent. However, the theory of scattering by an elastic sphere (Hickling, 1962) is now well established. Neubauer, Vogt and Dragonette (1974) have compared the theory with measurements on aluminium and tungsten carbide spheres, and the agreement is reasonable.

Theory

Steady State Theory

Consider a plane sine wave of constant amplitude travelling in the z-direction. Using spherical polar coordinates (Fig. 1) and the usual complex notation, the sound pressure is:

$$p_i\ (r, \theta, t) = p_o\ \exp\ (i\ \{\omega t - kr \cos\theta\}\ ) \quad \ldots\ldots\ldots\

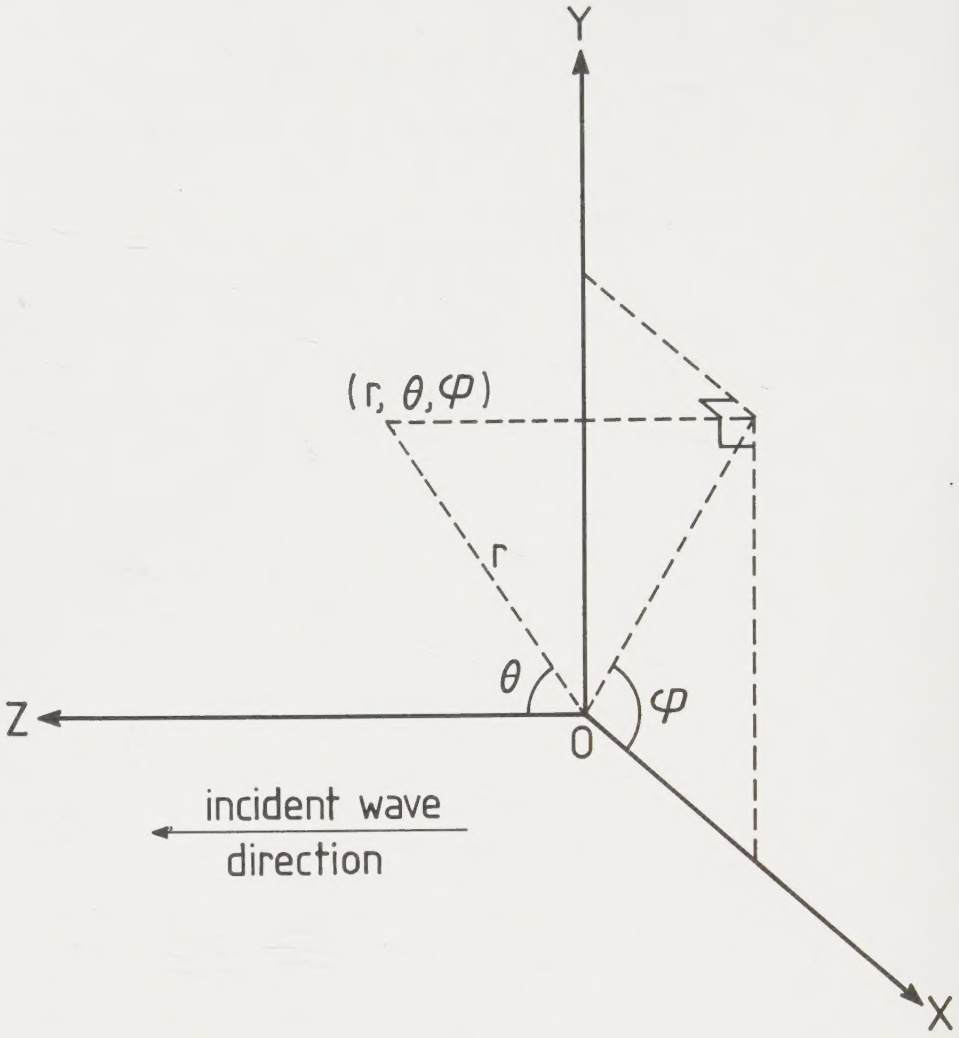

Figure 1. Spherical polar coordinates. The origin is at the centre of the spherical target.

when $\theta = \pi$, (2) gives the backscattered pressure. It is convenient to express this in terms of the "form function" $f_r(q)$, where q = ka and a is the radius of the sphere:

$$p_s\ (r, \pi, t) = p_o\ (a/2r)\ f_r\ (q)\ \exp\ (i\ \{\omega t - kr\}\ ) \quad \ldots\ldots\ldots\ldots\ldots\ldots\ldots\ldots\ldots\ldots (3)$$

The scattered field is determined from the solution of wave equations based on the classical theory of elasticity. Hickling (1962) has described the solution as a sum of partial waves:

$$p_{so}\ (r, \theta) = -\ p_o \sum_{\ell=o}^{\infty} (-i)^{\ell+1}\ (2\ell+1)\ \sin\eta_\ell\ \exp\ (i\ \eta_\ell)\ h_\ell\ (kr)\ P_\ell\ (\cos\theta)$$

$$\ldots\ldots\ldots\ldots\ldots\ldots\ldots\ldots\ldots\ldots\ldots\ldots\ldots\ldots\ldots\ldots\ldots\ldots\ldots\ldots (4)$$

$P_\ell\ (\cos\theta)$ is a Legendre polynomial and $h_\ell\ (kr)$ is a spherical Hankel function of the second kind, defined by

$$\left.\begin{aligned} h_\ell\ (x) &= j_\ell\ (x) - i\ y_\ell\ (x) \\ j_\ell\ (x) &= J_{\ell+\frac{1}{2}}\ (x) \sqrt{\ }\ (\pi/2x) \\ y_\ell\ (x) &= Y_{\ell+\frac{1}{2}}\ (x) \sqrt{\ }\ (\pi/2x) \end{aligned}\right\} - \quad \ldots\ldots\ldots\ldots\ldots\ldots\ldots\ldots\ldots\ldots\ldots\ldots\ldots\ldots\ldots\ldots\ldots\ldots\ldots\ldots (5)$$

where $J_{\ell+\frac{1}{2}}(x)$ and $Y_{\ell+\frac{1}{2}}(x)$ are Bessel functions of the first and second kinds respectively. Hickling's equations for η_ℓ contain typographical errors, so the equations are given in full below in a form convenient for programming.

Three sound velocities have to be considered. The velocity in water is c, and the velocities of longitudinal and transverse waves within the sphere are c_1 and c_2 respectively. If ρ is the density of water and ρ_1 is the density of the sphere, then:

$$q = ka\ ;\ q_1 = qc/c_1\ ;\ q_2 = qc/c_2 \quad \text{.....(6a)}$$

$$A_2 = (\ell^2 + \ell - 2)\, j_\ell(q_2) + q_2^2\, j''_\ell(q_2) \quad \text{.....(6b)}$$

$$A_1 = 2\ell(\ell+1)\,[q_1 j'_\ell(q_1) - j_\ell(q_1)] \quad \text{.....(6c)}$$

$$\alpha = 2(\rho_1/\rho)(c_2/c)^2 \quad \text{.....(6d)}$$

$$\beta = (\rho_1/\rho)(c_1/c)^2 - \alpha \quad \text{.....(6e)}$$

$$B_2 = A_2 q_1^2\,[\beta j_\ell(q_1) - \alpha j''_\ell(q_1)] - A_1 \alpha\,[j_\ell(q_2) - q_2 j'_\ell(q_2)] \quad \text{.....(6f)}$$

$$B_1 = q\,[A_2 q_1 j'_\ell(q_1) - A_1 j_\ell(q_2)] \quad \text{.....(6g)}$$

$$\tan\eta_\ell = -[B_2 j'_\ell(q) - B_1 j_\ell(q)]\ /[B_2 y'_\ell(q) - B_1 y_\ell(q)] \quad \text{.....(6h)}$$

The prime symbol denotes differentiation of the function with respect to the argument.

An important feature of the equations is that the physical properties of the sphere appear in ratio with corresponding properties of water, ie ρ_1/ρ, c_1/c and c_2/c. Thus the scattering is determined by these dimensionless ratios and by q which is the ratio of the sphere circumference to the sound wavelength in water.

In the far field, $kr >> 1$, the form function is:

$$f_\infty(q) = -(2/q) \sum_{\ell=0}^{\infty} (-1)^\ell (2\ell+1) \sin\eta_\ell \exp(i\eta_\ell) \quad \text{.....(7)}$$

The acoustic cross section σ is defined to be 4π times the far field backscattered intensity, normalised to r - 1m, divided by the incident wave intensity. For the elastic sphere:

$$\sigma = \pi a^2\ |\ f_\infty(q)|^2 \quad \text{.....(8)}$$

and the target strength in dB is:

$$TS = 10\ \mathrm{Log}_{10}\ (\sigma/4\pi) \quad \text{.....(9)}$$

The above theory applies when the incident wave source is far enough distant for the incident field in the vicinity of the target to be reasonably described as a plane wave. The case of a source near the target was discussed by Hickling (1962), but it will not be considered here. For calibration purposes, the distance between the target and the transducer should be large compared with both the target diameter and the wavelength, when the plane incident wave and the far field scattering approximations would be adequate.

Transient Theory

Practical sonars transmit pulses, not steady state waves, but a pulse may be described as a sum of steady state frequency components. Thus the scattered pulse waveform may be deduced from the sum of the scattered components of the incident pulse spectrum. Consider the following incident wave that is a modulated pulse having a rectangular envelope and a carrier frequency $\omega_o = q_o\ c/a$:

$$\left.\begin{aligned} p_i(\tau) &= p_o \exp(i\, q_o\, \tau) \text{ for } |\tau| < \tau_o/2 \\ p_i(\tau) &= 0 \text{ for } |\tau| >= \tau_o/2 \end{aligned}\right] \quad \ldots\ldots (10)$$

where τ is the transformed time parameter:

$$\tau = (ct - r\cos\theta)/a \quad \ldots\ldots (11)$$

The pulse duration is τ_o a/c. Noting that q is proportional to frequency, the pulse may be expressed as a Fourier integral:

$$p_i(\tau) = p_o \int_{-\infty}^{\infty} g(q) \exp(i\, q\, \tau)\, dq \quad \ldots\ldots (12)$$

where

$$g(q) = \frac{\sin(\{q-q_o\}\tau_o/2)}{\pi(q-q_o)} \quad \ldots\ldots (13)$$

The scattered field is obtained by integrating over the frequency components in the pulse spectrum (Hickling, 1962; Dragonette, Vogt, Flax and Neubauer, 1974). The far field backscattered pressure is:

$$p_{bf}(\tau_s) = p_o \frac{a}{2r} \int_{-\infty}^{\infty} f_\infty(q)\, g(q) \exp(i\, q\, \tau_s)\, dq \quad \ldots\ldots (14)$$

Where the form function for the elastic sphere target is given by (7) and τ_s is a second transformed time parameter:

$$\tau_s = (ct - r)/a \quad \ldots\ldots (15)$$

The Perceived Target Strength

Suppose that a signal v_i is applied to the transmitter input of a sonar system (Fig. 2), and that reflection from a target results in a signal v_o at the receiver output. The electrical signals v_i and v_o are measured, and their relationship depends upon the acoustic properties of the target. ω_o is the centre (tuned) frequency of the system, and $q_o = \omega_o\ a/c$.

If $v_i = V \exp(i\omega_o t)$, a steady state signal, then a calibration factor K_o is defined by the equation:

$$\sigma = K_o |v_o|^2 / |v_i|^2 \quad \ldots\ldots (16)$$

K_o depends upon system characteristics such as the transducer efficiency and the amplifier gains. The cross-section σ is given by (8) in the case of a spherical target.

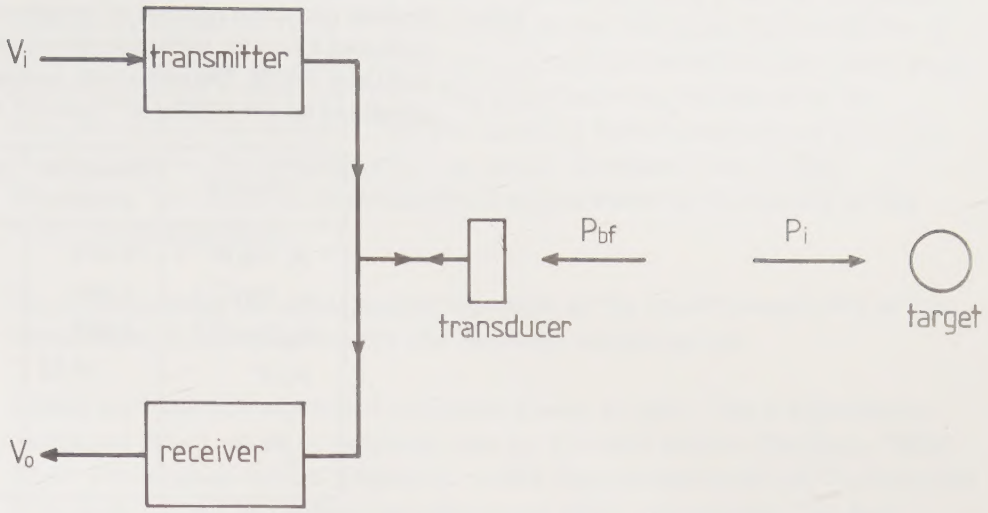

Figure 2. Elements of a sonar system.

The definition of σ given earlier is meaningful only for steady state signals. When v_i is transient, the intensities vary with time and another definition is required. A convenient parameter for the purpose is the "perceived cross-section", which is defined in terms of the ratio between output and input signal energies:

$$\sigma_p = K_o \left(\int_{t1}^{t2} |v_o|^2 dt \right) / \left(\int_{t3}^{t4} |v_i|^2 dt \right) \quad \text{.....(17)}$$

The integration limits are chosen to include the periods when the signals are significantly above noise level. σ_p depends upon the electrical characteristics of the sonar system as well as the acoustic properties of the target.

The electrical parts of the system are specified by two functions. $F(q)$ is the combined frequency response function of the transmitter and the transducer in transmit mode, normalised so that $F(q_o) = 1$. Similarly, $G(q)$ is the combined response function of the transducer in receive mode and the receiver circuits, and $G(q_o) = 1$.

If v_i is a pulse of carrier frequency ω_o and duration τ_o a/c, it can be shown that the perceived cross-section of the elastic sphere is:

$$\sigma_p = \pi a^2 \left(\int_{-\infty}^{\infty} |f_\infty(q) F(q) G(q) g(q)|^2 dq \right) / \left(\int_{-\infty}^{\infty} |g(q)|^2 dq \right) \quad \text{.....(18)}$$

where $f_\infty(q)$ and $g(q)$ are given by (7) and (13). As the pulse length tends to infinity:

$$\sigma_p \rightarrow \pi a^2 |f(q_o)|^2 \quad \text{.....(18a)}$$

Thus σ_p in the limiting case of steady state signals is consistent with σ as previously defined.

By analogy with (9), the perceived target strength is defined as:

$$TSp = 10 \text{ Log}_{10} (\sigma_p / 4\pi) \quad \text{.....(19)}$$

Table I. Physical properties relevant to the target strength of spheres. The densities are measured values for particular spheres and the sound velocities are from Kaye and Laby (1973). The ratios with corresponding properties of water have been calculated for $\rho = 1030 kg\ m^{-3}$ and $c = 1490 m\ s^{-1}$

Material	Tungsten carbide	Stainless steel	Brass
ρ_1 (kg m^{-3})	14,860	7,970	8,360
c_1 (m s^{-1})	6,655	5,980	4,372
c_2 (m s^{-1})	3,984	3,297	2,100
ρ_1/ρ	14.43	7.74	8.12
c_1/c	4.47	4.01	2.93
c_2/c	2.67	2.21	1.41

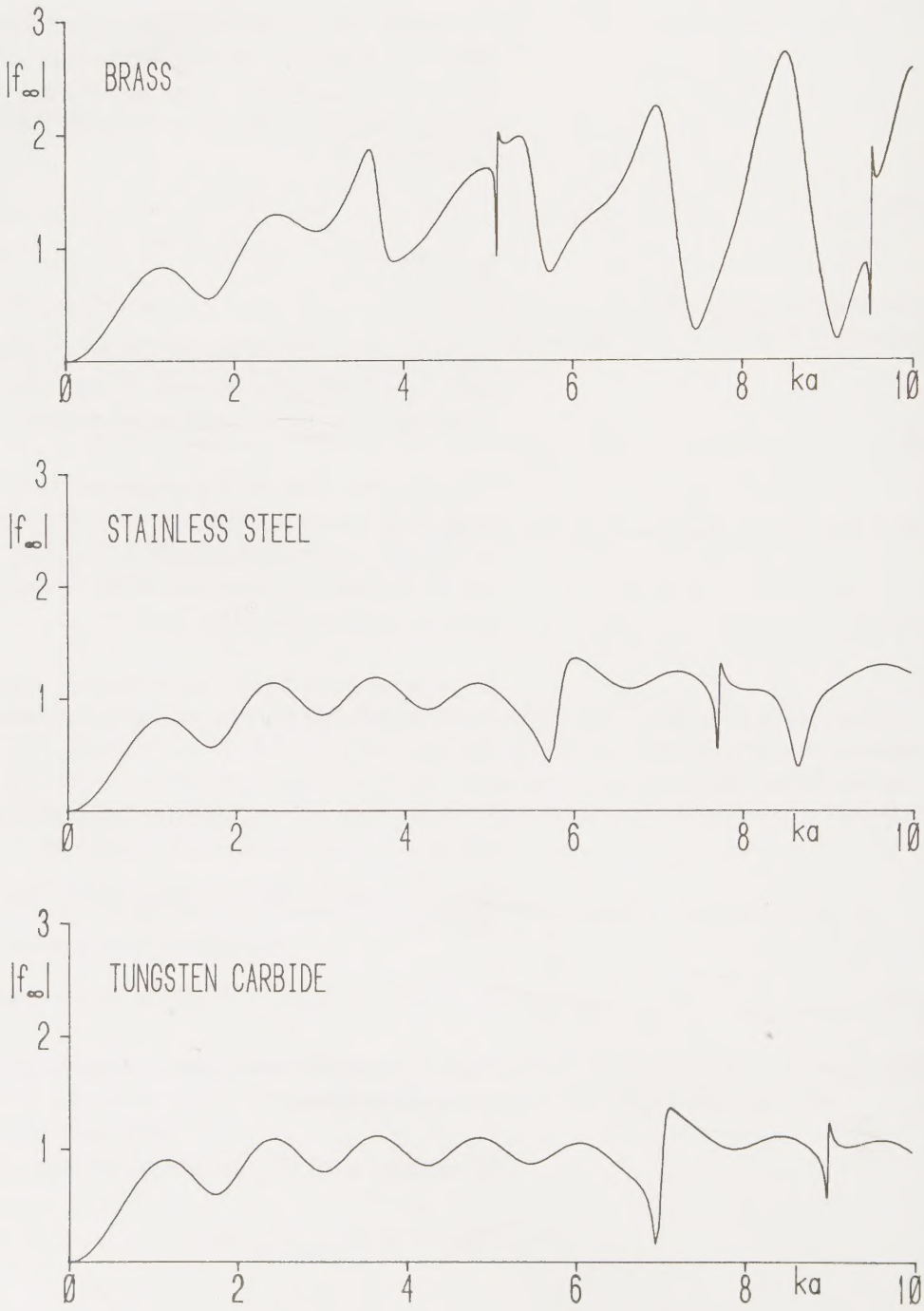

Figure 3. Form functions for three alloys. The functions have been calculated using the property ratios shown in Table I.

Results

Acoustic Cross-Sections

The density and sound velocity ratios for brass, stainless steel and tungsten carbide are shown in Table I. These ratios define the scattering properties of homogeneous spheres, in particular the acoustic cross-section for steady state scattering which is given by (6-8). The equations may be evaluated by standard numerical methods, and the resulting form functions are shown in Figure 3 against the parameter $q = ka$, which is proportional to the frequency. The acoustic cross-section is proportional to the square of the form function modulus.

For each material the cross-section increases as the fourth power of q at low frequencies, in accordance with the Rayleigh scattering law.

Above $q = 1$ the form function oscillates slowly at first. This is a geometric resonance effect which is exhibited also by the rigid sphere (Rudgers, 1969). Then, above some critical frequency, much sharper oscillation of the function is evident, caused by mechanical resonances within the sphere. The first mechanical resonance occurs at $q = 3.6$, 5.7 and 6.9 for brass, stainless steel and tungsten carbide respectively. The frequencies of the mechanical resonances are sensitive to small changes particularly in c_2 (Neubauer *et al.*, 1974). Such changes might occur for example through work hardening or temperature variation. To obtain a stable target strength, therefore, the first mechanical resonance frequency should be well above the carrier frequency ω_o of the sonar. This implies that for a given ω_o spheres larger than a certain size will be unsuitable as standard targets. Among the materials considered here, the size limit is greatest for tungsten carbide and smallest for brass. Conversely, for a particular sphere, there is a maximum ω_o above which the sphere is unsuitable as a standard target.

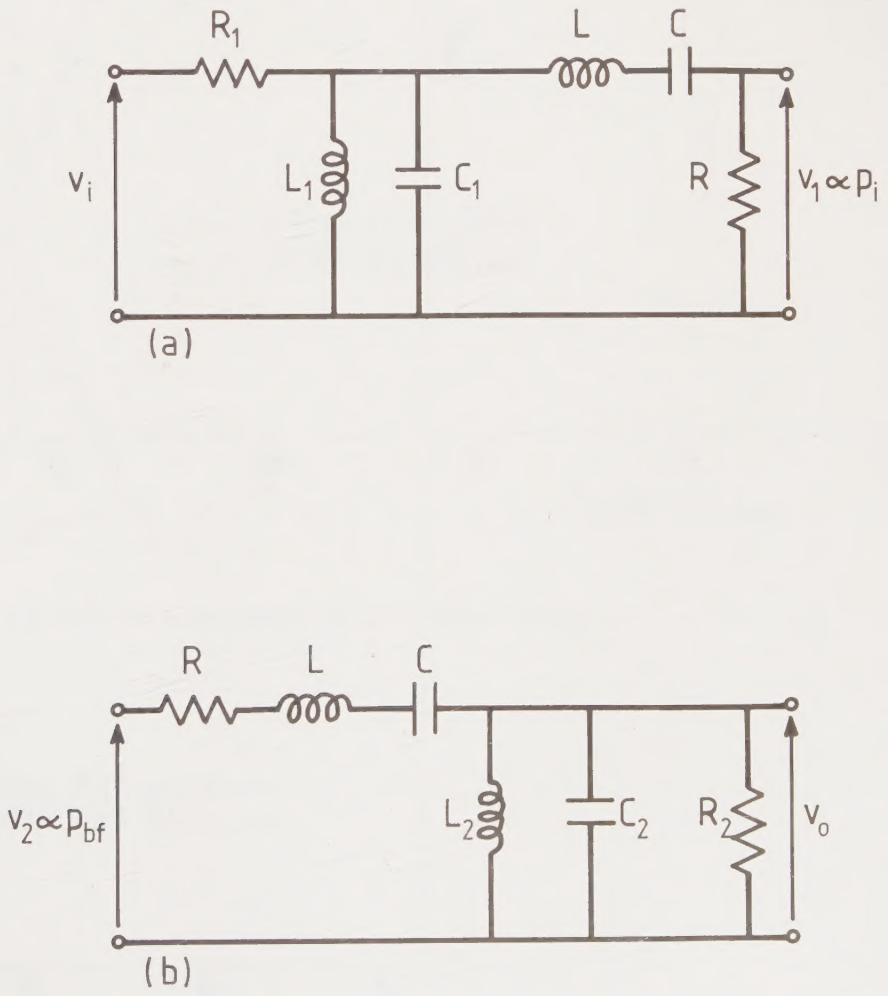

Figure 4. Equivalent circuits for a sonar system with a transformer coupled transmitter — (a) transmitter and transducer in transmit mode, (b) transducer in receive mode and tuned receiver.

System Characteristics

Consider a sonar system with a transformer coupled transducer for which simplified equivalent circuits are shown in Figure 4. The transducer is represented by the inductance L and the capacitance C. R is the radiation resistance and the quality factor of the transducer is $Q = L\omega_o/R$. If reciprocity is assumed, L, C and R are the same in transmit and receive modes. The system is matched so that the input and output resistances are the same ($R_1 = R_2 = R$), and the reactive components are tuned to the operating frequency of the sonar; thus $L_1 C_1 = L_2 C_2 = LC$.

The transfer functions of this sytem are:

$$F(q) = (1 - \tfrac{1}{2}QQ_1 X^2 + \tfrac{1}{2}i \{Q + Q_1\} X)^{-1} \quad \ldots\ldots (20)$$

$$G(q) = (1 - \tfrac{1}{2}QQ_2 X^2 + \tfrac{1}{2}i \{Q + Q_2\} X)^{-1} \quad \ldots\ldots (21)$$

where $X = (q/q_o - q_o/q)$, $Q_1 = L_1 \omega_o/R_1$ and $Q_2 = L_2 \omega_o/R_2$

The particular system considered here represents a 38kHz sonar that has been used for fish target strength experiments (Forbes, Simmonds and Edwards, 1980). For that system $Q = 8.1$, $Q_1 = 1.27$ and $Q_2 = 10.77$. These values have been derived from electrical measurements and the response of the system to short acoustic pules in water.

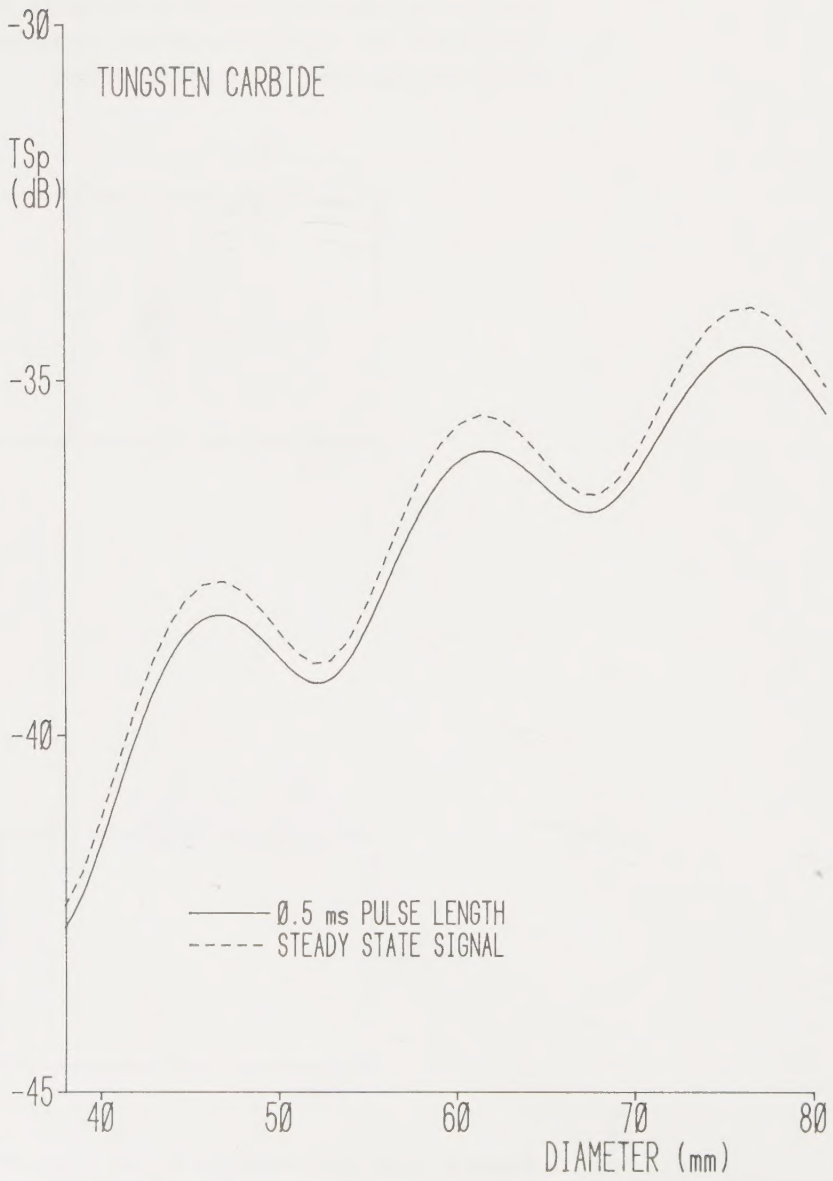

Figure 5. Perceived target strength of tungsten carbide spheres.

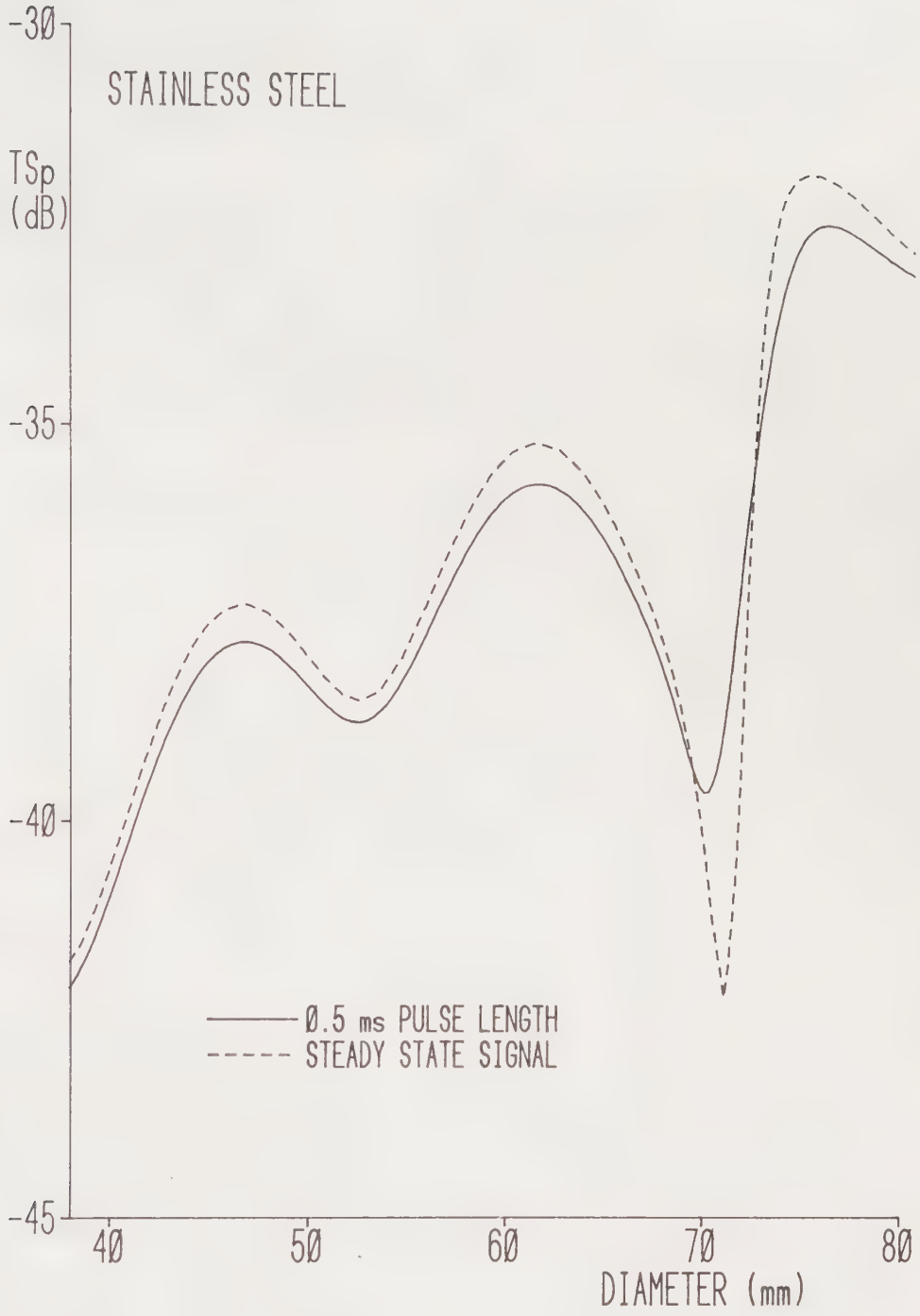

Figure 6. Perceived target strength of stainless steel spheres.

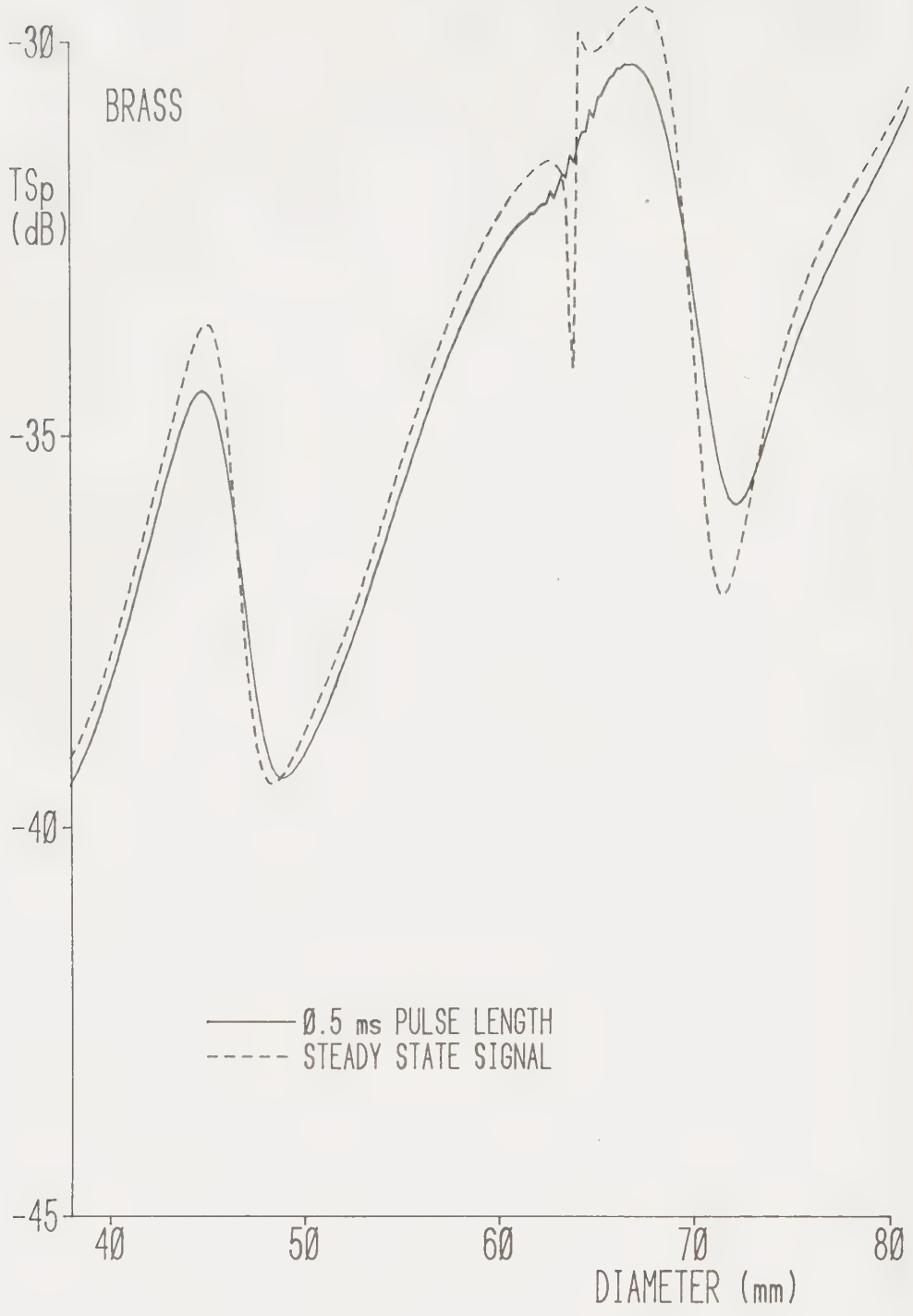

Figure 7. Perceived target strength of brass spheres.

Perceived Target Strengths

The perceived target strength (TSp) is obtained from the form function and equations (18-21). Figures 5-7 show how TSp varies with the sphere size, assuming that the material properties are those given in Table I. The calculations have been performed for the sonar system described above and a pulse length of 0.5ms. Results for an infinite pulse length (steady state signal) are shown for comparison. In the latter case, TSp is equal to the target strength as defined by (9) and it is independent of the system characteristics.

More detailed calculations have been performed for three spheres which have been used or considered for use as standard targets. They are (1) a tungsten carbide ball bearing, (2) a stainless steel sphere supplied by Simrad as a calibration target and (3) a brass sphere which has been used by the Marine Laboratory as a "sub standard" target. The densities quoted in Table I are measured values for these spheres; however, the sound velocities in that table are taken from published data (Kaye and Laby, 1973). The sphere sizes are given in Table II together with the calculated TSp for various pulse lengths.

Table II. The perceived target strengths of three spheres when insonified by 38kHz pulses of duration T. The results have been evaluated for the material properties given in Table I and the particular sonar system described in the text

Material	Tungsten carbide	Stainless steel	Brass
Diameter (mm)	38.1	60.0	69.9
q_o	3.05	4.81	5.60
T(ms)	TSp (dB)	TSp (dB)	Tsp(dB)
0.5	−42.66	−35.90	−33.15
1.0	−42.49	−35.64	−33.43
2.0	−42.42	−35.52	−33.59
3.0	−42.40	−35.48	−33.65
∞	−42.34	−35.40	−33.76

The sensivity of TSp to small changes in various parameters has been investigated. For the first two spheres, the effect of varying the carrier frequency by 500Hz and the material property ratios by 10% is shown in Figures 8-9. The changes in TSp are fairly small, around 0.1dB for the tungsten carbide sphere and 0.2dB for the stainless steel sphere.

Equivalent results for the brass sphere are shown in Figure 10. Here the variation of TSp is considerable, especially the variation with c_2/c, which is an order of magnitude greater than that exhibited by the other spheres. The reason is that 38kHz is close to one of the mechanical reasonances of the sphere. As stated earlier, the resonance frequencies are sensitive to small changes in c_2/c. In view of this, the TSp estimates for the brass sphere will be useful only if c_2/c is accurately known. The direct measurement of c_2 in a sphere is difficult. However, when the acoustic carrier frequency is close to a mechanical resonance, the scattered pulse shape has certain features which depend upon c_2. Thus c_2 may be estimated indirectly by comparing observed and calculated pulse shapes.

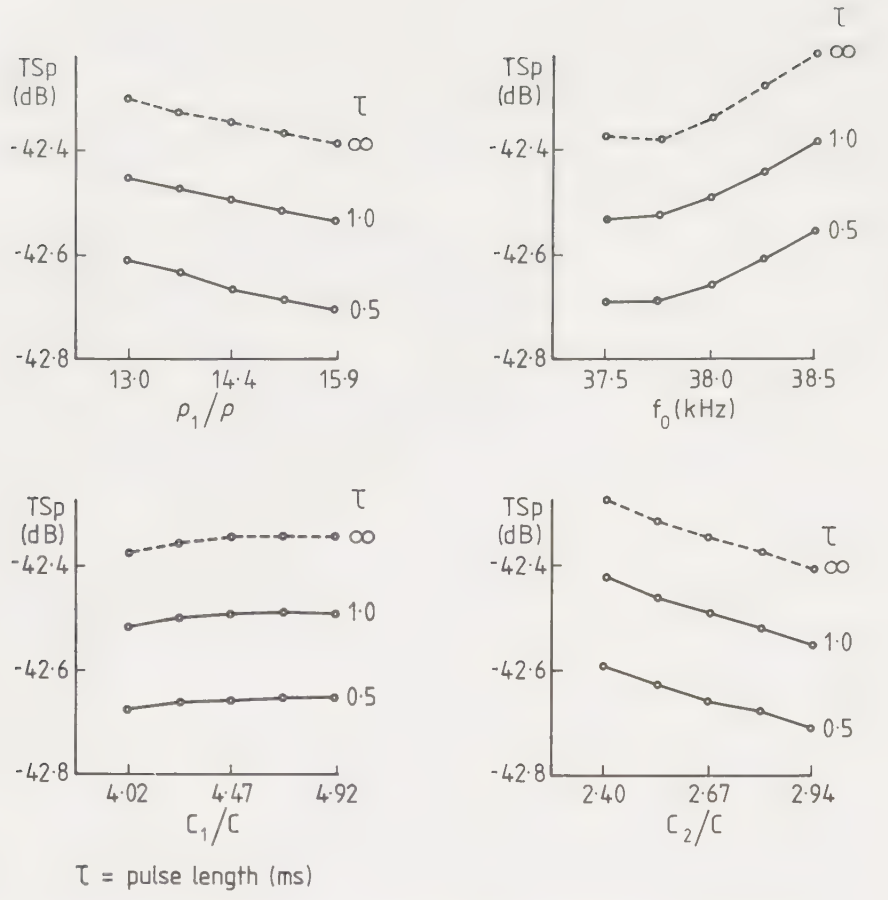

Figure 8. Variation of TSp for a 38.1mm diameter tungsten carbide sphere.

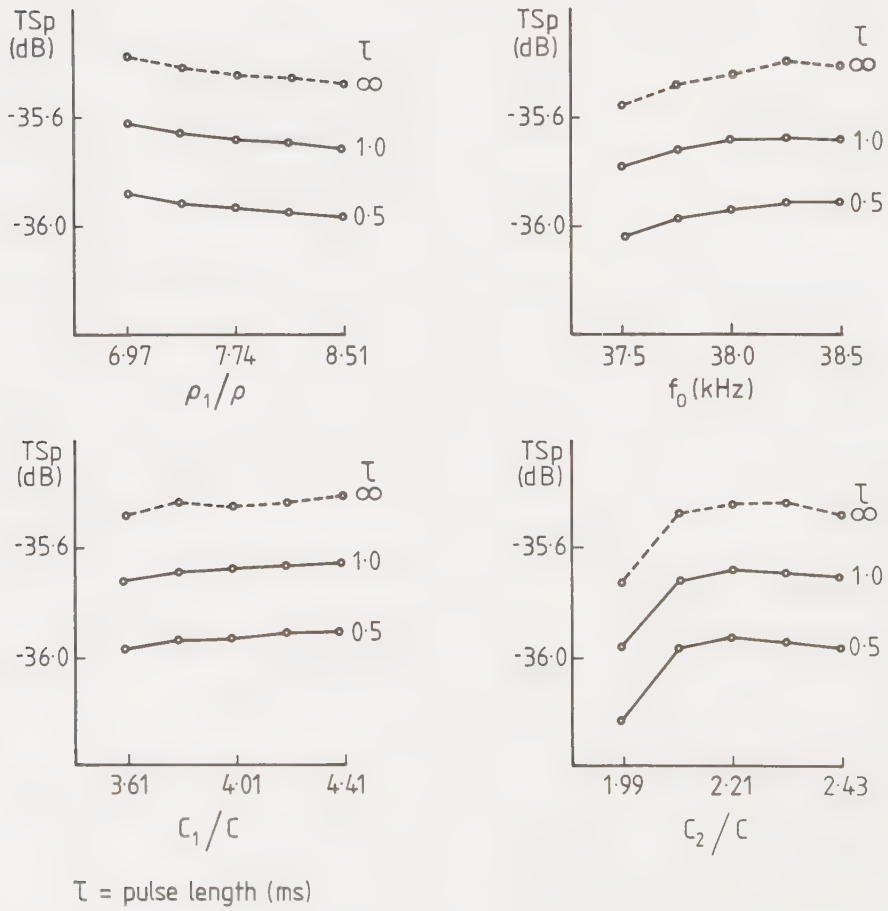

Figure 9. Variation of TSp for a 60mm diameter stainless steel sphere.

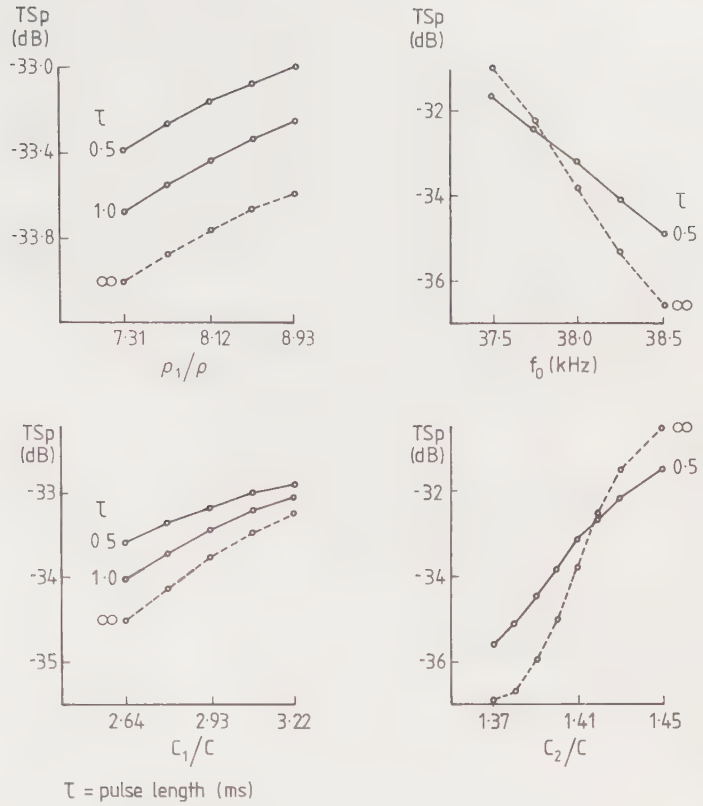

Figure 10. Variation of TSp for a 69.9mm diameter brass sphere.

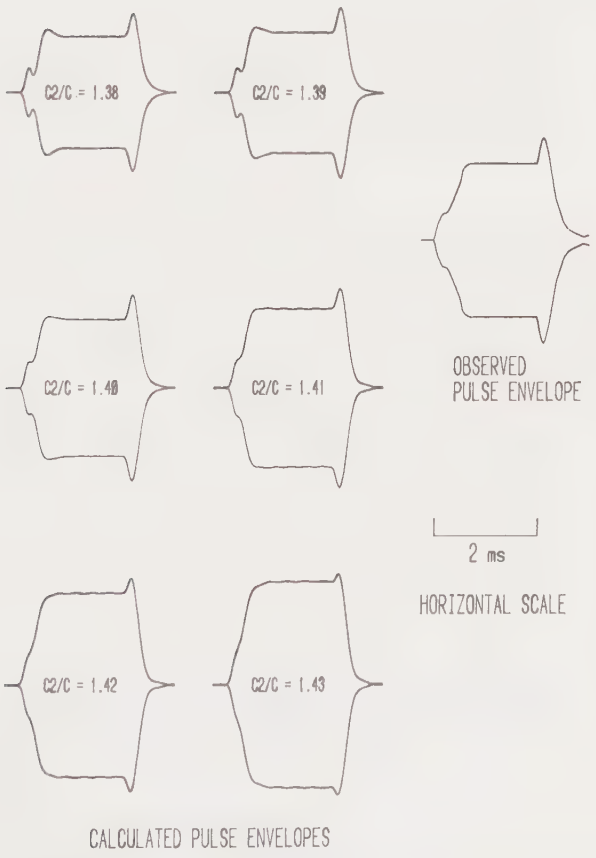

Figure 11. Comparison of observed and calculated pulse envelopes at the receiver output when a 2ms long 38kHz pulse is applied to the transmitter input and the target is a 69.9mm diameter brass sphere. The vertical scale is arbitrary.

Figure 11 shows the envelope of the receiver output voltage observed on an oscilloscope when the brass sphere is insonified by a 2ms transmitted pulse. The envelope has two well-defined characteristics, the inflextion on the leading edge and the ring on the trailing edge. The calculated waveform is obtained from an equation similar to (14) but including the factors F(q) and G(q) within the integral. Received pulse envelopes have been so calculated for a series of c_2/c values and the results are presented in Figure 11. The observed and the calculated pulse shapes are significantly different except for $c_2/c = 1.41$, when they are in close agreement. The results indicate that c_2/c is within the range 1.41 ± 0.01, confirming the value that was obtained originally from published data.

The received pulse shape does not change much with c_1/c, and this parameter cannot be estimated by the same technique. However, it seems reasonable to allow the same proportional error in both the sound velocity parameters, and in any case the error in c_2/c is much the more important. It is now possible with the aid of Figure 10 to set limits on the perceived target strength estimates for the brass sphere. For example, for 0.5ms pulses, $TSp = -33.2 \pm 0.7$dB. Wider limits apply at longer pulse lengths and for steady state signals, $TSp = -33.8 \pm 1.4$dB.

The limits on the TSp estimates for the tungsten carbide sphere are less than ± 0.1dB for sound velocity parameters within ± 10% of the assumed values. Variation of the sphere density and the carrier frequency need not be considered since precise measurements of these parameters are easily obtained and the TSp estimates may be corrected if necessary.

According to Kaye and Laby (1973) the sound velocities for mild, hardened and stainless steels lie within ± 2% of the values shown in Table I. There is no reason to suppose that greater differences should occur between materials in the stainless steel group, but it is suggested that limits of ± 5% on the assumed sound velocity ratios would cover any variation likely to arise in practice. The corresponding limits on the TSp estimates for the 60mm stainless steel sphere are then ± 0.2dB derived from the results in Figure 9.

The possibility of error in the system transfer functions has not been considered so far. The equivalent circuits used to derive these functions (Fig. 4) approximate the performance of real transducers. For example, secondary resonances of the transducer are not taken into account. The significance of the system frequency response is indicated by the difference Δ TS between the steady state and the 0.5ms pulse length curves in Figures 8-10. Since 0.5ms is the shortest pulse length that would be used with such a sonar, corresponding to the broadest spectrum, error in the transfer functions would contribute some proportion of ΔTS to the uncertainty in TSp. However, given measurements of the system characteristics using standard techniques, it is considered that the transfer functions can be defined well enough to reduce such errors to insignificance.

Conclusions

The target strength of solid spheres depends upon the carrier frequency, the diameter and the density of the sphere. These parameters may be obtained from simple measurements, but the target strength also depends upon the sound velocities in the solid, which are less easy to measure. However, if the carrier frequency is well below the first mechanical resonance, the target strength is insensitive to the sound velocities. Calculations may then be based on published data for the sound velocities and the variation consequent upon the normal range of alloy composition is not significant.

38kHz is the sonar frequency normally used on fish surveys. For calibration purposes, reference targets are required to have a TSp at this frequency around −42dB or higher. This implies a minimum sphere diameter around 40mm. The larger the sphere, the lower are the mechanical resonance frequencies. There is therefore a maximum diameter which should not be exceeded for reference targets to have satisfactory acoustic properties. For the 60mm diameter stainless steel sphere which has been studied in some detail, the first mechanical resonance occurs at 45.1kHz. Satisfactory results were obtained for this sphere, but the use of larger stainless steel spheres is not recommended. The corresponding diameter limit for tungsten carbide spheres is 72mm. Brass is not considered to be a suitable material for reference targets, since the mechanical resonance frequencies are relatively low.

The acoustic properties of tungsten carbide have been shown to be superior to those of stainless steel. The advantage is marginal however, and stainless steel is much the cheaper material.

The calculation method outlined in this paper has been used to estimate the target strength of a 60mm stainless steel sphere to within ± 0.2dB, and that of a 38.1mm tungsten carbide sphere to within ± 0.1dB, at 38kHz. This is a higher precision than would be practical from a direct measurement using calibrated hydrophones.

For the quantitative assessment of fish stocks, it is the signal appearing at the sonar output which has to be measured and calibrated. The target strength as normally defined describes only the properties of the target, but the observed echo from a pulsed sonar also depends upon the system frequency response. To overcome this difficulty, the system performance is described by the "perceived" target strength, which is proportional to the observed energy in the sonar output signal. Thus the perceived target strength is a property of the complete system, the sonar as well as the target. The definition of TSp in terms of the observed energy is particularly suited to the calibration of echo integrator equipment.

Summary

One method of calibrating sonars is to measure the echo from a standard target. The calibration accuracy depends upon knowledge of the acoustic properties of the target. The theory of acoustic scattering by solid spheres is used to calculate the target strength of brass, stainless steel and tungsten carbide spheres. The scattering is highly frequency dependent and the "perceived target strength" (TSp) is defined, which takes account of the frequency response of the target, transducer and electronics. The sonar is modelled by equivalent circuits and the variation of TSp with pulse length and the physical properties of the target material is examined. In order for the target to have well-defined reflecting properties, the lowest mechanical resonance should occur well above the acoustic carrier frequency. In the case of 38kHz sonars, it is found that brass is not a suitable material for standard targets, that tungsten carbide is excellent but stainless steel is also satisfac-factory. Calculations and simple measurements will allow the perceived target strength to be determined more precisely than is practical by direct acoustic measurement.

References

Dragonette, L.R., Vogt, R.H., Flax, L. and Neubauer, W.G. 1974
Acoustic reflection from elastic spheres and rigid spheres and spheroids. II Transient analysis. *Journal of the Acoustical Society of America,* **55**(6), 1130-1137.

Forbes, S.T., Simmonds, E.J. and Edwards, J.I. 1980.
Progess in target strength measurements on live gadoids. Marine Laboratory Working Paper No. 80/15, 40 pp. (mimeo).

Hickling, R. 1962.
Analysis of echoes from a solid elastic sphere in water. *Journal of the Acoustical Society of America,* **34** (10), 1582-1592.

Kaye, G.W.C. and Laby, T.H. 1973.
Tables of Physical and Chemical Constants (14th ed.). London, Longman, 386 pp.

Neubauer, W.G., Vogt, R.H. and Dragonette, L.R. 1974.
Acoustic reflection from elastic spheres. *Journal of the Acoustical Society of America,* **55** (6), 1123-1129.

Rudgers, A.J. 1969.
Acoustic pulses scattered by a rigid sphere immersed in a fluid. *Journal of the Acoustical Society of America,* **45** (4), 900-910.

Urick, R.J. 1967.
Principles of Underwater Sound for Engineers. New York, McGraw-Hill, 342 pp.

Welsby, V.G. and Hudson, J.E. 1972.
Standard small targets for calibrating underwater sonars. *Journal of Sound and Vibration,* **20**, 399-406.

Appendix 1
List of Principal Symbols

a	sphere radius
c	sound velocity in water
c_1	longitudinal sound wave velocity
c_2	transverse sound wave velocity
$f_r(q)$	backscattering form function
$F(q)$	transmit mode transfer function
$g(q)$	pulse spectrum
$G(q)$	receive mode transfer function
$h_\ell(kr)$	spherical Hankel function of the second kind
k	wave number in water (2π / wavelength)
ℓ	partial wave mode number
p_i	incident pressure field
p_o	incident pressure amplitude
p_s	scattered pressure field
p_{so}	scattered pressure amplitude
p_{bf}	far field backscattered sound pressure
$P_\ell(\cos\theta)$	Legendre polynomial
q	dimensionless frequency parameter (ka)
q_o	value of q at the carrier frequency
Q, Q_1, Q_2	equivalent circuit quality factors
r	radial position coordinate
t	time
TS	target strength
TSp	perceived target strength
v_i	transmitter input signal
v_o	receiver output signal
θ	angular position coordinate
η_ℓ	partial wave phase angle
ρ	water density
ρ_1	sphere density
σ	backscattering cross-section
σ_p	perceived backscattering cross-section
τ	incident wave transformed time
τ_s	scattered wave transformed time
ω	frequency
ω_o	carrier frequency

1980

No. 18. Changes in the Respiration and Blood Circulation of Cod, *Gadus morhua* L., induced by Exposure to Pollutants.
By A.D.F. Johnstone and A.D. Hawkins, 18 pp.

1981

No. 19. Survey of Trace Elements in Fish and Shellfish landed at Scottish Ports 1975-76.
By I.M. Davies, 28 pp.

No. 20. A Study of the Sand Clouds Produced by Trawl Boards and their Possible Effect on Fish Capture .
By J. Main and G.I. Sangster, 20 pp.

No. 21. Orientation and Energetic Efficiency in the Offshore Movements of Returning Atlantic Salmon *Salmo salar* L.
By G.W. Smith, A.D. Hawkins, G.G. Urquhart and W.M. Shearer, 22 pp.